THE MELTING PERFORMANCE BLAST FURNACE SLAGS WITH HIGH ALUMINA CONTENT

H.-Y. Zheng [a, b, *], Y. Zhang [a, b], Z. Wang [a, b], J.-L. Du [c], X. Jiang [a, b], Q.-J. Gao [a, b], F.-M. Shen [a, b]

[a] Key Laboratory for Ecological Metallurgy of Multimetallic Mineral (Ministry of Education), Northeastern University, Shenyang, P. R. China
[b] School of Metallurgy, Northeastern University, Shenyang, P. R. China
[c] Steelmaking Operations Department, Shougang Jingtang United Iron & Steel Co., Ltd., Tangshan, P. R. China

Abstract

With a view to understanding the performance of the blast furnace slag with high Al_2O_3 content, the effects of $w(MgO)/w(Al_2O_3)$, $w(CaO)/w(SiO_2)$, and $w(Al_2O_3)$ on the melting performance (melting characteristic temperature and melting heat) of the blast furnace slag with high Al_2O_3 content were investigated by the differential scanning calorimeter (DSC) method. Experimental results indicate that melting end temperature (T_{end}) for almost all the slags has no obvious change with the increase of $w(MgO)/w(Al_2O_3)$, $w(CaO)/w(SiO_2)$ and $w(Al_2O_3)$ of the slag will raise T_{end} of the slag. When $(w(MgO)/w(Al_2O_3))$, R, and $w(Al_2O_3)$ are high, the melting onset temperature (T_{onset}) of the slag increases with the increase of any variables. When $w(CaO)/w(SiO_2)$ is low, T_{onset} of the slag decreases with the increase of $w(Al_2O_3)$. $w(MgO)/w(Al_2O_3)$, $w(CaO)/w(SiO_2)$, and $w(Al_2O_3)$ within the scope of this study and all these factors lead to the increase of the slag melting heat.

Keywords: High alumina blast furnace slag; Melting characteristic temperature; Melting heat; Differential scanning calorimetry; Raman spectrum analysis

1. Introduction

In the process of blast furnace smelting, the melting performance (melting index and melting heat) of the blast furnace slag plays a crucial role in smooth operation, high yield, cost reduction of pig iron, and longevity of blast furnace [1-5]. In general, the melting temperature is the lowest temperature at which the solid phase disappears completely during the melting process of the slag and it corresponds to the liquidus temperature in the phase diagram. During the blast furnace smelting process, the slag is required to have an appropriate melting temperature for ensuring a smooth operation of the blast furnace with low energy consumption [6, 7].

Up to now, the blast furnace smelting process uses a large amount of imported ore, which results in a high Al_2O_3 content ($w(Al_2O_3)$) in the slag [8-10]. And the ratio of $w(MgO)$ to $w(Al_2O_3)$ ($w(MgO)/w(Al_2O_3)$) has been gaining attention [11-14]. However, almost all research focused on the melting performance of the slags with low alumina [15-18] and reports on the melting performance of high alumina blast furnace slags by thermogravimetry-differential scanning calorimeter (TG-DSC) are rare [19-22]. Therefore, the effects of slag compositions, including $w(MgO)/w(Al_2O_3)$, basicity (R), and $w(Al_2O_3)$, on the melting performance (melting onset temperature, final melting temperature, and melting heat) and microstructure were investigated by using DSC in this paper. The results will have a practical guiding significance in blast furnace smelting with high alumina.

2. Experimental

In this paper, the melting performance (melting index and melting heat) of CaO-SiO_2-Al_2O_3-MgO slag during melting was determined by using TG-DSC. By using the analyses of the phase diagram, XRD, SEM-EDS, and Raman spectroscopy, the influence mechanism of mineral evolution and composition on melting performance and microstructure of slag during heating up was discussed.

2.1. Determination of the melting performance

Differential scanning calorimetry (DSC) is a technique for measuring the energy added to a sample

and reference as a function of temperature and the obtained DSC curve is typically used for quantitative analysis. There are three main characteristics for the molten slags based on the DSC curve, 1) melting onset temperature (T_{onset}), 2) final melting temperature (T_{end}), and 3) melting heat (enthalpy change ΔH or heat of fusion).

Figure 1 is a schematic diagram of a DSC curve and the melting performance is illustrated. Among them, T_{onset} of the slag refers to the temperature at the intersection of the extrapolated baseline and the tangent to the maximum slope of the opposite transition curve, and T_{end} of the slag corresponds to the intersection of the extrapolated baseline and the tangent at the maximum slope of the curve corresponding to the end of the transition, as shown in Figure 1(a). The area of the endothermic peak in Figure 1(b) is defined as the melting heat of the slag, which can be determined with equation (1). According to the abovementioned method, the melting performance of the melting onset and end temperatures of the slag and the melting heat can be determined based on the DSC curve of the slag.

$$\Delta H = K \int_{0}^{\tau} \Delta T d\tau \qquad (1)$$

where "K" is a constant, which is the heat transfer coefficient between the sample and the heating device, and determined by the physical parameters of the device, "ΔH" is the heat of fusion, "ΔT" is the temperature difference between reference and sample, and "τ" is the testing time.

2.2. Experimental procedure

According to the actual composition of blast furnace slag, a pre-melted quaternary slag system with $w(CaO) + w(MgO) + w(SiO_2) + w(Al_2O_3) = 100\%$ was prepared at 1450°C for 30 min or longer using a graphite crucible. After being quenched the glassy sample (15mg) is grounded into powder (smaller than 74 μm) for measuring the melting performance. The synchronous thermal analyzer

(STA, Germany, Netzsch STA409CD) was used for measuring the thermogravimetry-differential scanning calorimetry (TG-DSC) curve because it offers good reproducibility and high resolution at elevated temperatures. Figure 2 shows the temperature program, which included 15 mins preparing time at 30°C for putting the sample into a Pt crucible, 150 mins heating time from 30°C to 1500°C with a heating rate of 10 K/min, and then holding time at 1500°C for 10 mins. In a typical measuring experiment, the powder sample was about 15mg and argon (Ar) was used as the protecting atmosphere and the gas flow was set as 50 mL/min. Repeated measurements show that the experimental error is less than 5%.

3. Experimental results and discussion

In the metallurgical process, the slag of melting temperature, viscosity, and abilities of desulfurization and alkali discharge are determined by basicity ($R=w(CaO)/w(SiO_2)$) [23-25]. Therefore, R is a very important practical parameter representing the composition of the slag, and it is also one of the important bases for determining the slagging system of the blast furnace. The ratio of $w(MgO)$ to $w(Al_2O_3)$ ($w(MgO)/w(Al_2O_3)$), which has been gaining attention recently, was introduced for estimating the slag in this
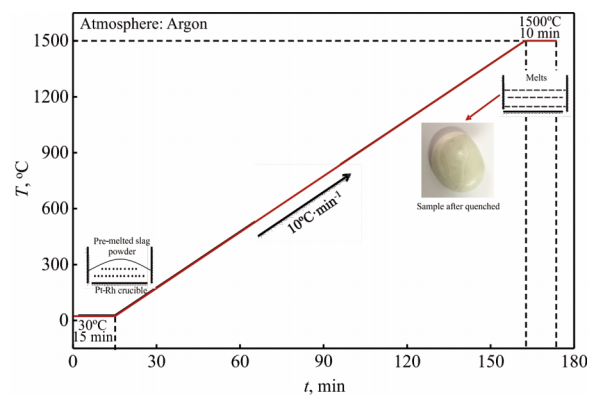

Figure 2. *Temperature program for measuring the melting performance*
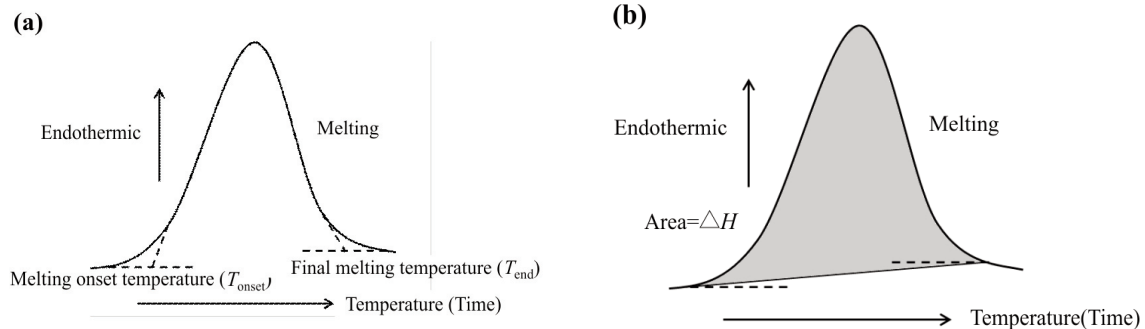

Figure 1. *The schematic diagram for the melting performance (a) Melting index, (b) Melting heat (ΔH)*

study because the negative effect of Al_2O_3 on the slag performance will be weakened by adding MgO into the slag when Al_2O_3 content in the slag is high. Therefore, the effects of the slag compositions ($w(MgO)/w(Al_2O_3)$=0.25–0.45, R=1.15–1.25, and $w(Al_2O_3)$ =15–20%) on the melting performance (melting index and melting heat) of the blast furnace slag with high Al_2O_3 content were investigated in this study.

3.1. Phases analysis in the slag

To get a preliminary understanding of the slag composition, CaO-SiO_2-MgO-Al_2O_3 pseudo-quaternary melts with $w(Al_2O_3)$=15% and $w(Al_2O_3)$=20% are plotted with Factsage 7.30 in Figure 3. The slag composition investigated in this study is the points in Figure 3 and its main component is melilite (Mel, $Ca_2(Al, Mg)[(Al, Si)SiO_7]$), which is mainly a complex solid solution composed of gehlenite (Gh, $Ca_2Al(Al, Si)_2O_7$, $T_{mel.}$=1593°C) and

akermanite (Ak, $Ca_2MgSi_2O_7$, $T_{mel.}$=1450°C). According to Figure 3, it is found that the slag with a liquidus temperature lower than 1400°C is only R=1.15, $w(MgO)/w(Al_2O_3)$=0.25, and $w(Al_2O_3)$=15%.

To understand the slag structure, the scanning electron microscope energy dispersive spectrometer (SEM-EDS, Japan, HITACHI S-4800) was introduced. The slag with R=1.25, $w(MgO)/w(Al_2O_3)$=0.45, and $w(Al_2O_3)$=20% was kept at 1350°C for 1 hour and then quenched. Melilite (Mel, $Ca_2(Al, Mg)[(Al, Si)SiO_7]$) is confirmed as shown in Table 1.

Furthermore, the slags with R=1.25, $w(MgO)/w(Al_2O_3)$=0.45 at 800°C and 1000°C were quenched to get the structure of the slag at high temperature and analyzed by X-ray diffraction analyzer (XRD, Japan, Rigaku Ultima IV). Figure 4 shows the XRD analysis results of the slags. As shown in Figure 4, the minerals in the blast furnace slag are mainly melilite (Mel, $Ca_2(Al, Mg)[(Al, Si)SiO_7]$) and are in good agreement with the phase diagram in Figure 3.
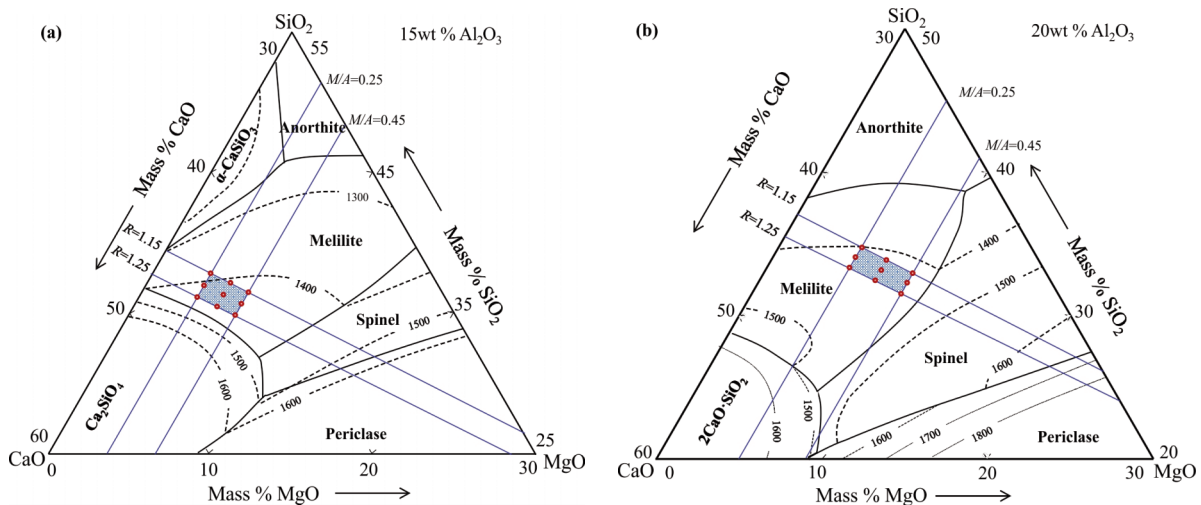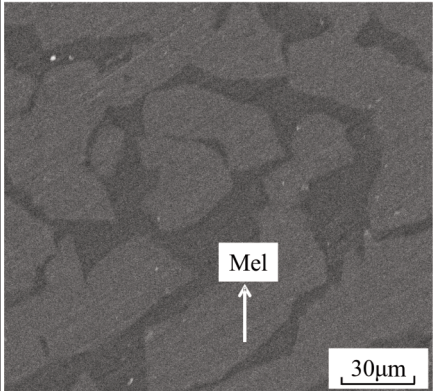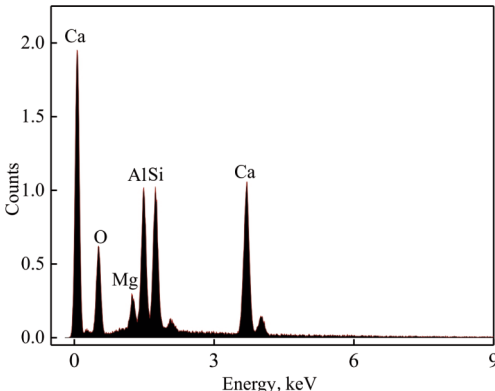

Figure 3. *Phase diagram of CaO-SiO_2-Al_2O_3-MgO melts (a) $w(Al_2O_3)$=15%, (b) $w(Al_2O_3)$=20%*

Table 1. *SEM-EDS of slag*

SEM morphology	Energy spectrum	Element analysis	
		Element	Atomic%
		O	44.14
		Ca	26.20
		Mg	3.16
		Al	12.15
		Si	14.12
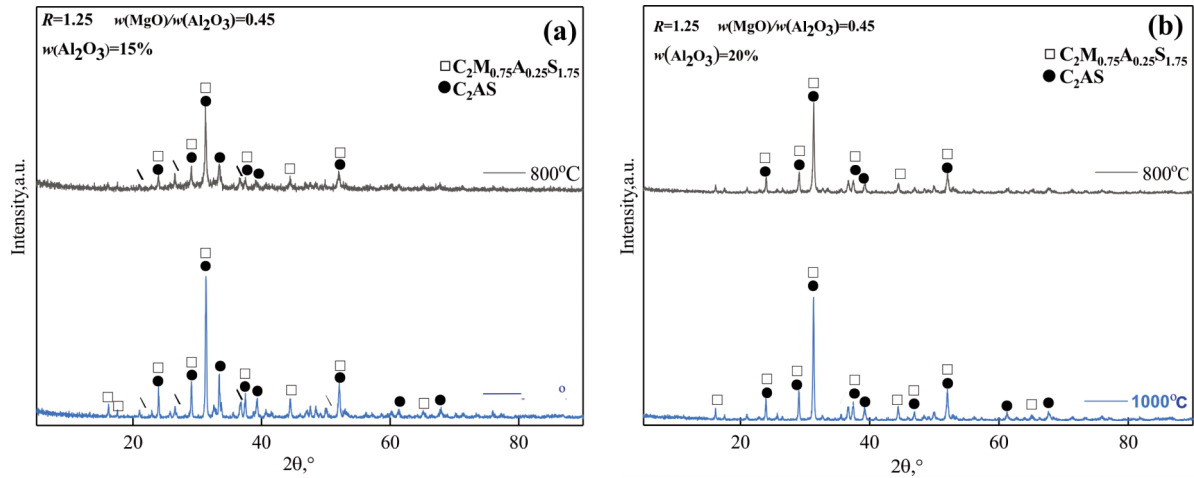
Figure 4. XRD analysis results of slags (R=1.25, w(MgO)/w(Al₂O₃)=0.45)
(a) w(Al₂O₃)=15%, (b) w(Al₂O₃)=20%

3.2. DSC curves

Figure 5 is the DSC curves of the BF slag. All curves show exothermic peaks between 891–944℃ (Peak 1, average temperature is 920℃). Exothermic peaks are caused by phase transitions from amorphous SiO_2 to crystal SiO_2 with $\Delta H<0$. Most of the DSC curves show a sharp endothermic peak at 1282–1303℃ (Peak 3, average temperature is 1290℃), which is considered to be caused by the reverse eutectic reaction of Wo + Gh ↔ Liquid+ $\Delta H>0$. The peak at 1388–1447℃ (Peak 3, average temperature is 1409℃) is blunter than the endothermic peak at 1290℃, which is assumed as the endothermic peak of the melting process for the residual slag.
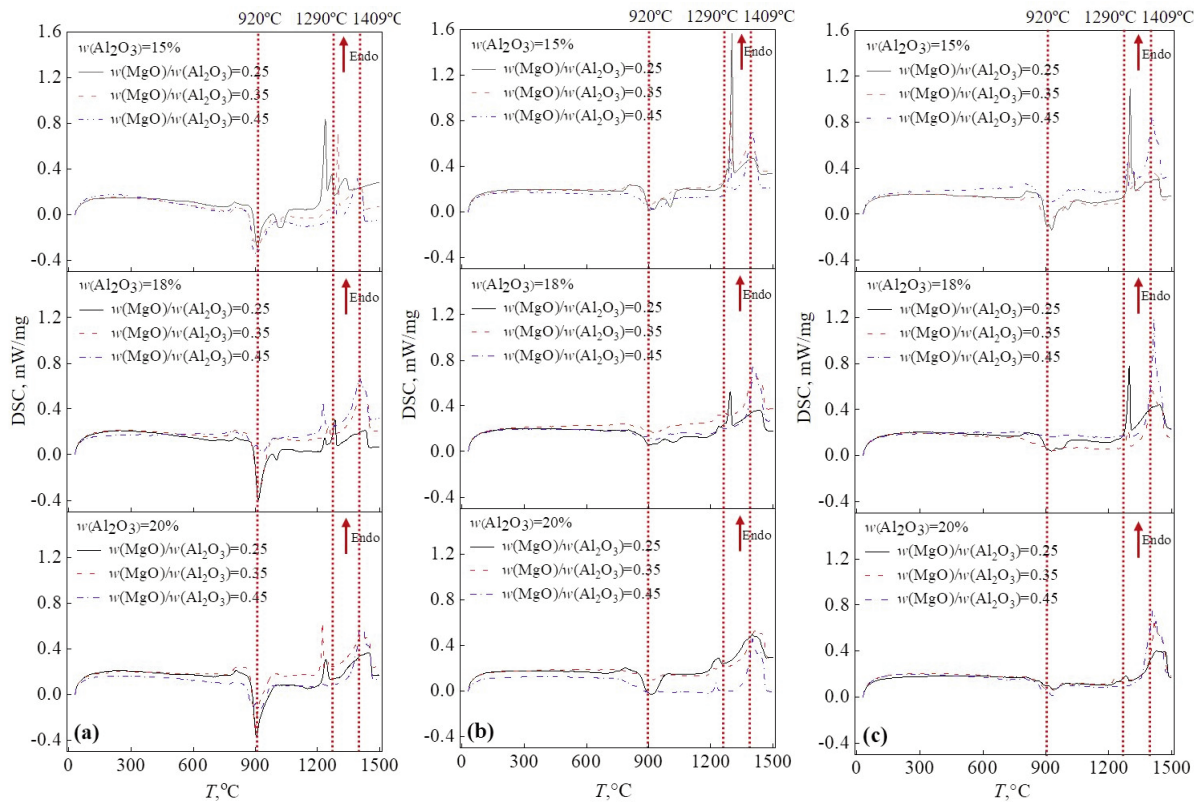

Figure 5. DSC curves of the slags
(a) R=1.15, (b) R=1.20, and (c) R=1.25

3.3. Effect of w(MgO)/w(Al₂O₃) on the melting performance

Figure 6 shows the effect of $w(MgO)/w(Al_2O_3)$ on the melting index (T_{onset}: melting onset temperature; T_{end}: final melting temperature). As shown in Figure 6. T_{end} of the slags except for $R=1.15$, $w(MgO)/w(Al_2O_3)=0.25$, and $w(Al_2O_3)=15\%$ has no obvious change because the compositions of the slags in this study are nearly similar. The liquidus temperature lower than 1400°C is only the slag of $R=1.15$, $w(MgO)/w(Al_2O_3)=0.25$, and $w(Al_2O_3)=15\%$, which is in good agreement with the phase diagram in Figure 2.

T_{onset} of the slag have no obvious change with the increase of $w(MgO)/w(Al_2O_3)$ when R and $w(Al_2O_3)$ in the slags are low (Figures 6(a) and 6(b)). However, T_{onset} of the slags increases with the increase of $w(MgO)/w(Al_2O_3)$ in Figure 6(c) when R and

$w(Al_2O_3)$ in the slags are high and it is a series of complex compounds with high melting point, such as spinel (Spl, MgO·Al₂O₃, $T_{mel.}$=2135°C) and forsterite (Fo, 2MgO·SiO₂, $T_{mel.}$=1890°C), are formed.

In order to verify whether high melting point compounds are generated in the slag with high R and $w(Al_2O_3)$, the slag of $R=1.25$, $w(MgO)/w(Al_2O_3)=0.45$, and $w(Al_2O_3)=20\%$ was prepared by keeping at 1350°C for 1 hour and then quenched for analysis by SEM-EDS. Spinel (Spl, MgO·Al₂O₃, $T_{mel.}$=2135°C) at Point A was founded as shown in Table 2 and the above supposition for the generation of high melting point compounds was confirmed.

Figure 7 illustrates the effect of $w(MgO)/w(Al_2O_3)$ on the melting heat. As $w(MgO)/w(Al_2O_3)$ increases, the melting heat of the slag increases as well. Typically, CaO and MgO act as a network modifier, and ions of Ca²⁺ and Mg²⁺ destroy the bridge oxygen
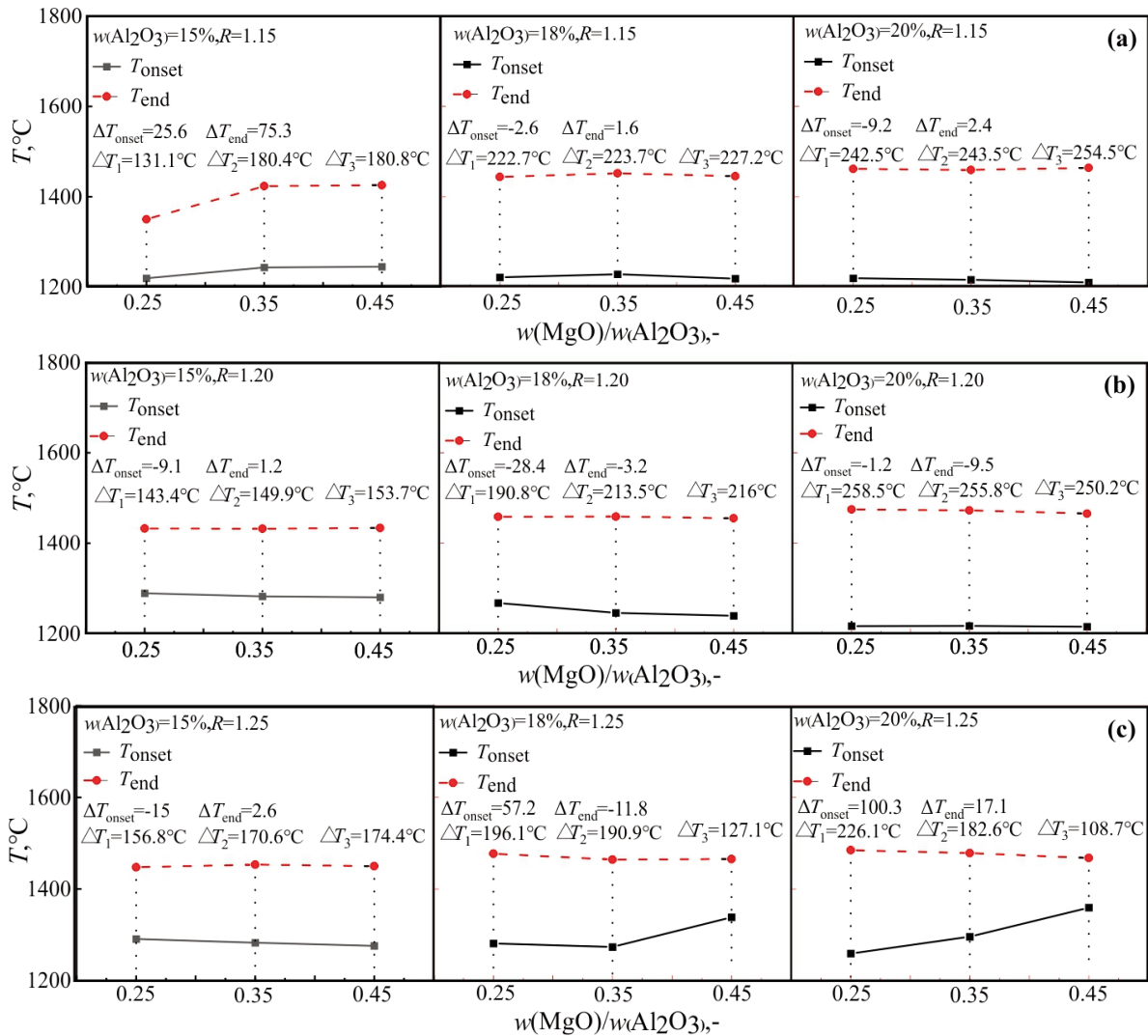

Figure 6. *Effect of w(MgO)/w(Al₂O₃) on melting index(a) R=1.15, (b) R=1.20, (c) R=1.25*

connecting in $[SiO_4]^{4-}$ tetrahedron and $[AlO_4]^{5-}$ tetrahedron, which results in the depolymerization of the complex network structure of the aluminosilicate and reduce the degree of polymerization of the slag [26-29]. As $w(MgO)/w(Al_2O_3)$ increases, more MgO replaces CaO in the slag to simplify and depolymerize the silicate network. It is noted that the lattice energy of MgO (3791 kJ/mol) is higher than the CaO lattice energy (3401 kJ/mol) [30]. Thus, the energy required to destroy the MgO lattice during the slag melting is higher than that of CaO and it results in an increase in melting heat. Meanwhile, complex compounds with high melting temperature, such as spinel (Spl. $MgO·Al_2O_3$, $T_{mel.}$=2135°C) and forsterite (Fo, $2MgO·SiO_2$, $T_{mel.}$=1890°C), are generated, and lead to a higher melting heat of the slag when $w(MgO)/w(Al_2O_3)$ increases.

3.4. Effect of R on the melting performance

Figure 8 shows the effect of R on melting index. As shown in Figure 8, it is found that the melting onset temperature of the slag, especially for the slag with high $w(Al_2O_3)$, and $w(MgO)/w(Al_2O_3)$, generally increases with the increase of R. It is because the melting temperature of CaO ($T_{mel.}$=2570°C) is higher than the melting temperature of SiO_2 ($T_{mel.}$=1723°C). In addition, it is found that the final
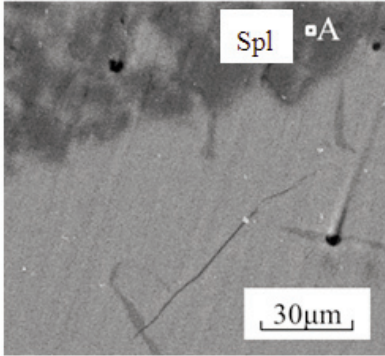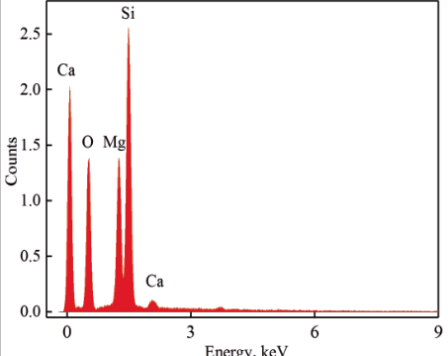
melting temperature slightly increases with the increase of R when $w(Al_2O_3)$ and $w(MgO)/w(Al_2O_3)$ are constant. It is considered that increasing R of the slag rises the liquidus temperature of the slag, which is in agreement with the phase diagram in Figure 3.

Figure 9 shows that the melting heat increases with the increase of R, and it is in agreement with the phase diagram in Figure 3. Because increasing R of the slag rises the liquidus temperature of the slag, i.e., increasing R of the slag rises the melting heat.

3.5. Effect of $w(Al_2O_3)$ on the melting performance

Figure 10 shows that the melting onset temperature decreases with the increase of $w(Al_2O_3)$ when R is low (R=1.15, 1.20). It is considered that the main reason is the slag composition (Mel, $2CaO·0.5MgO·0.5Al_2O_3·1.5SiO_2$) with low SiO_2 is near a eutectic line (1235–1250°C) and the slag undergoes a eutectic reverse reaction (equation (2)) along the eutectic line when An ($CaO·Al_2O_3·2SiO_2$) exist locally in the slag based on our previous work [31]. Thus, the process of liquid phase formation occurs at about 1250°C or lower temperature and the melting onset temperature gradually decreases with the increase of $w(Al_2O_3)$.

Table 2. *SEM-EDS results of the slag*

SEM morphology	Energy spectrum	Element analysis	
		Element	Atomic%
		O	59.17
		Ca	0.27
		Mg	13.92
		Al	26.59
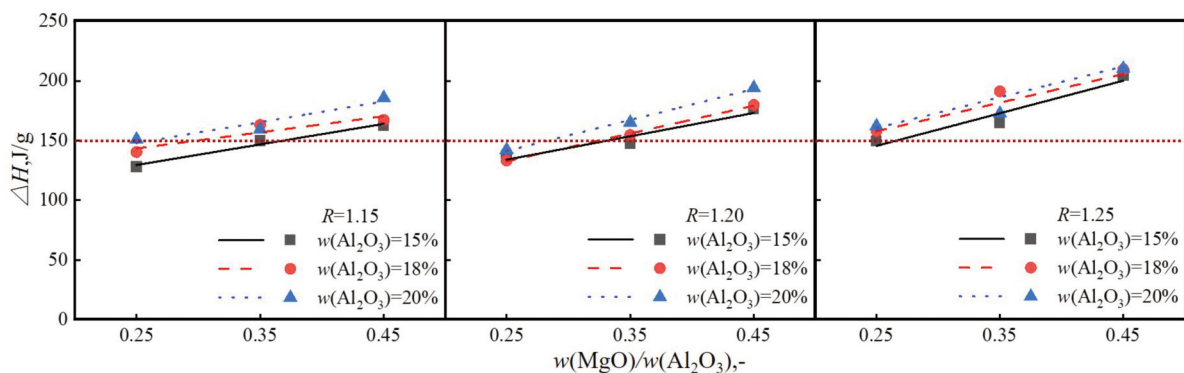
Figure 7. *Effect of $w(MgO)/w(Al_2O_3)$ on the melting heat*
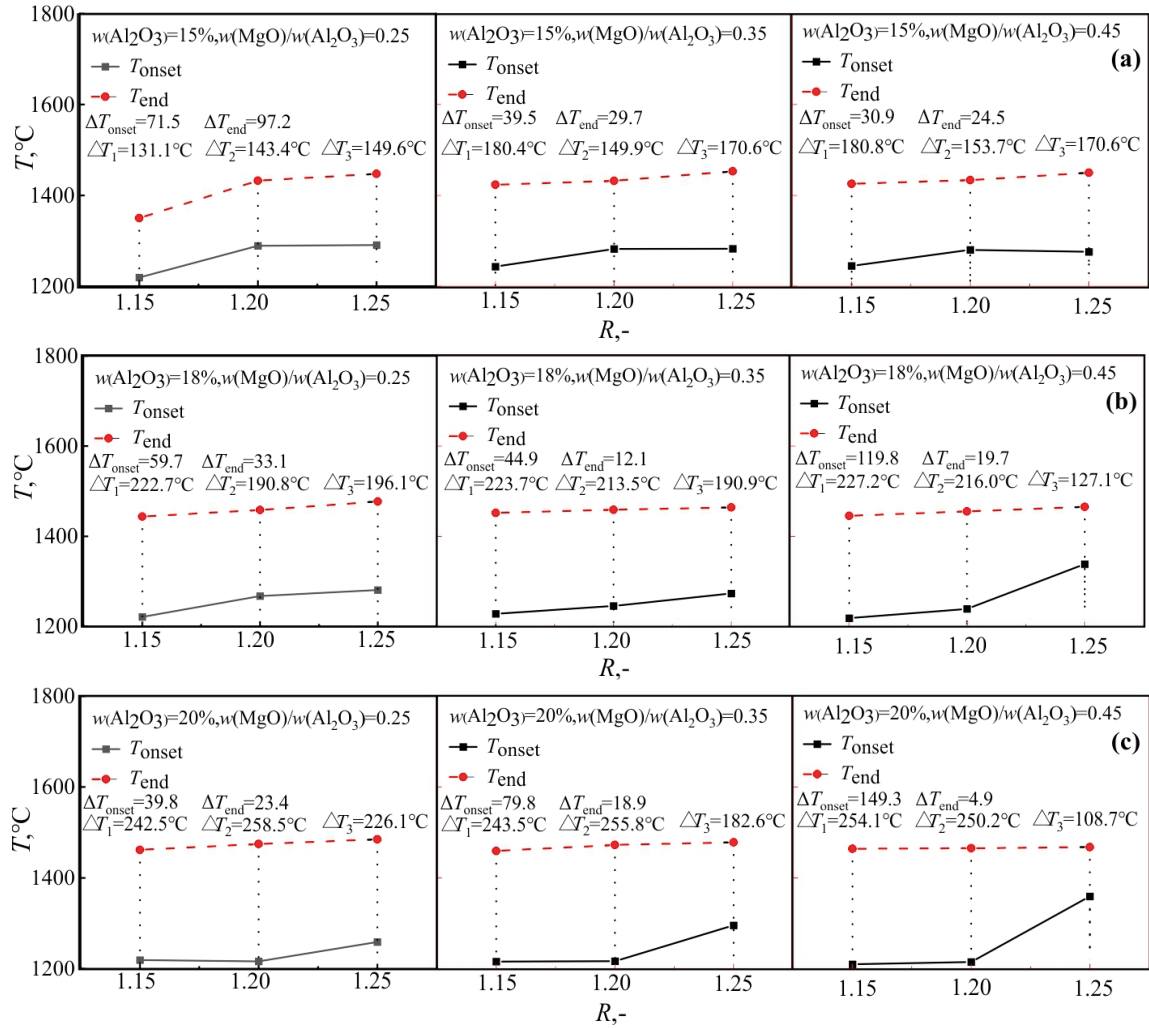
Figure 8. *Effect of R on melting index*
(a) w(Al_2O_3)=15%, (b) w(Al_2O_3)=18%, (c) w(Al_2O_3)=20%
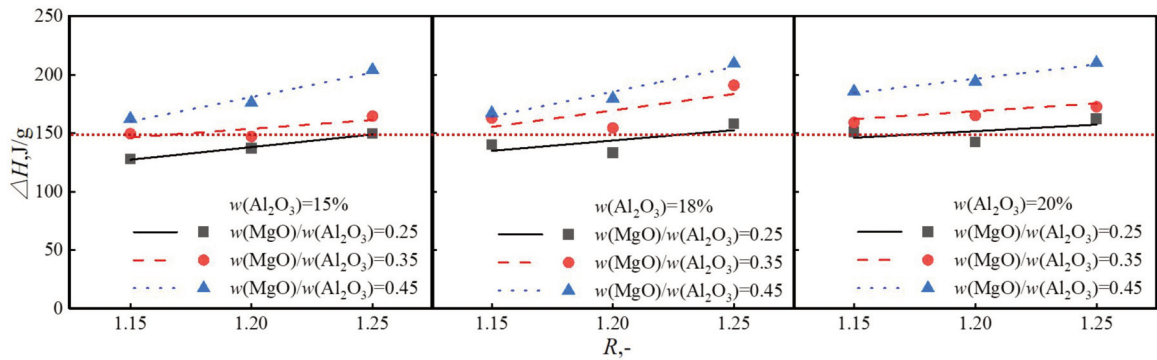
Figure 9. *Effect of R on the melting heat*

$$L \leftrightarrow CaO \cdot Al_2O_3 \cdot 2SiO_2 (An) + 2CaO \cdot$$
$$0.5MgO \cdot 0.5Al_2O_3 \cdot 1.5SiO_2 (Mel) \quad (2)$$
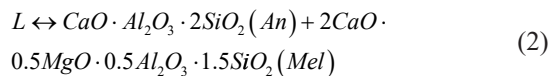
where L is the liquid phase, An is anorthite, Mel is melilite, and $\leftrightarrow$ indicates that the reaction is a reversible reaction.

However, when R=1.25, w(MgO)/w(Al_2O_3)=0.45, the melting onset temperature increases with the increase of w(Al_2O_3) and it is primarily due to the generation of certain high melting point compounds, such as spinel (Spl, MgO·Al_2O_3, $T_{mel.}$=2135°C). The high melting point compound leads to a poor fluidity

of the slag. Therefore, as the $w(Al_2O_3)$ in the slag increases, the internal structure due to the generation of high melting point compounds becomes complicated and the melting onset temperature of the slag increases.

The final melting temperature of the slag slightly increases with the increase of $w(Al_2O_3)$. It is assumed that the composition of the slag shifts to spinel and liquidus temperature increases with the increase of $w(Al_2O_3)$ as shown in Figure 3.

Figure 11 shows that the melting heat of the slag gradually increases with the increase of $w(Al_2O_3)$ in blast furnace slag under fixed R and $w(MgO)/w(Al_2O_3)$, which means that the slag needs more energy to depolymerize the network structure of the slag with the increase of $w(Al_2O_3)$ in the blast furnace slag. Figure 12 shows the Raman spectra of the CaO-SiO$_2$-Al$_2$O$_3$-MgO slag system at 1450ºC by using the Raman spectrometer (Shanghai, Renishaw, inVia Qontor) when the $w(Al_2O_3)$ is 15% and 18%,

respectively. It is found that with the increase of $w(Al_2O_3)$, $w(SiO_2)$ decreases, the spectral peak intensity of $[AlO_4]^{5-}$ cluster structure gradually increases (the degree of polymerization increases), the spectral peak intensity of $[SiO_4]^{4-}$ cluster structure gradually decreases (the degree of polymerization decreases). This indicates that with the increase of $w(Al_2O_3)$, part of $[SiO_4]^{4-}$ (Si^{4+}) is replaced by $[AlO_4]^{5-}$ (Al^{3+}) and the simple $Al_xO_y^{z-}$ structure with non-bridging oxygen in the slag polymerizes and transforms into a more complex $[AlO_4]^{5-}$ cluster structure (aluminosilicate structure) with bridging oxygen.

Furthermore, it is noted that Al$_2$O$_3$ is an ionic compound and its lattice energy is about 15111 kJ/mol [32], which is higher than the lattice energy of SiO$_2$ (2600 kJ/mol) [30]. Thus, the energy required to destroy Al$_2$O$_3$ lattice during the slag melting is quite higher than that of the SiO$_2$ lattice, which results in an increase in the melting heat when $w(Al_2O_3)$ increases.
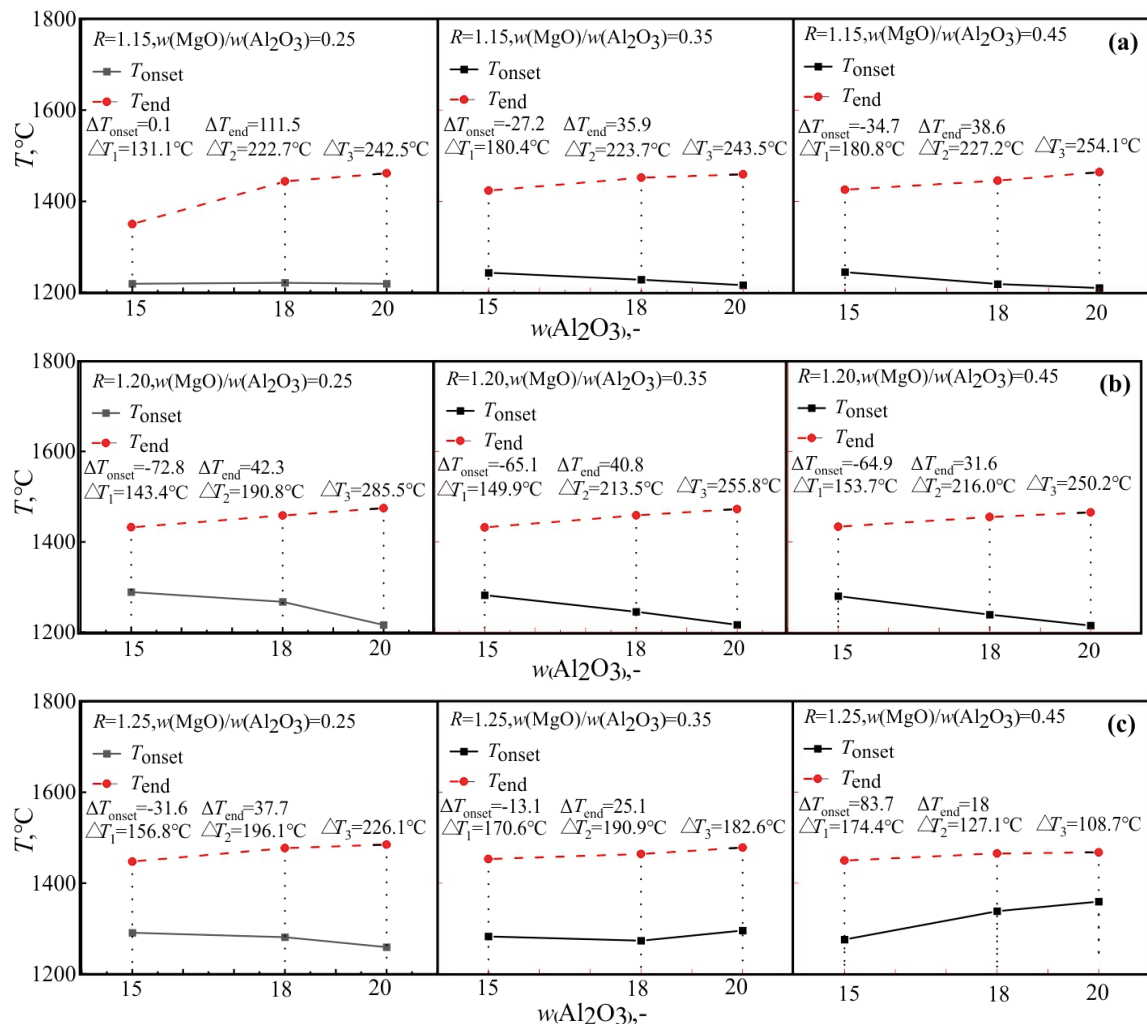

Figure 10. Effect of Al$_2$O$_3$ content on melting index
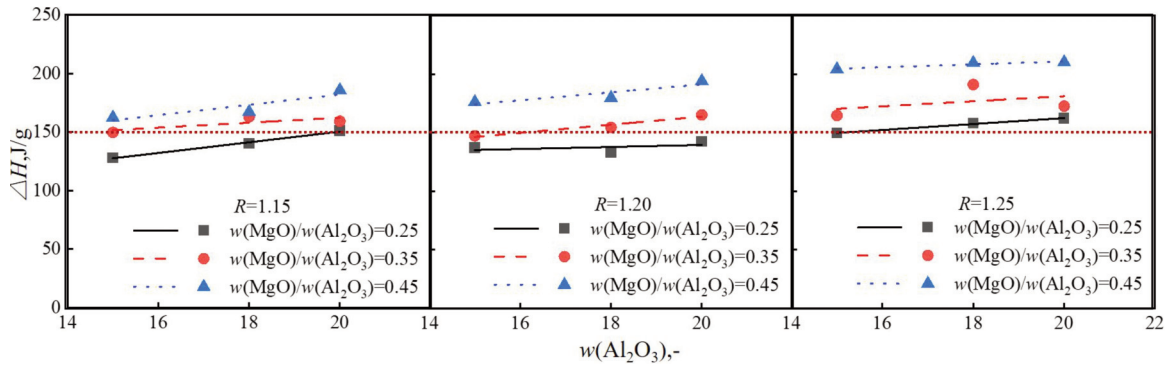*(a) R=1.15, (b) R=1.20, (c) R=1.25*

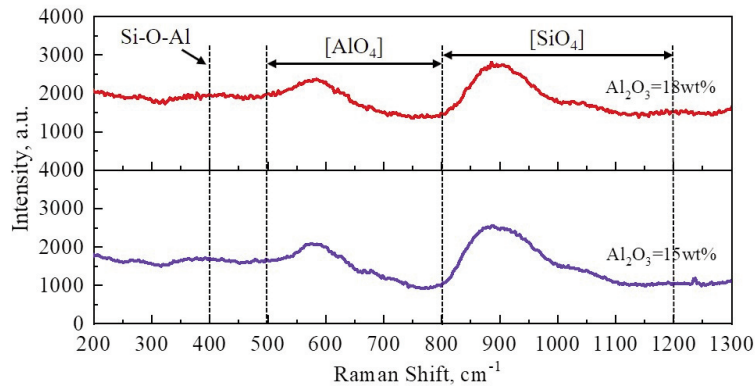**Figure 11.** *Effect of w(Al$_2$O$_3$) on the melting heat*

Figure 12. *Raman spectra of CaO-SiO$_2$-Al$_2$O$_3$-MgO melt at 1450°C (R=1.25)*

The melting heat of the actual slag was also measured by using the DSC method and between 160 J/g and 220 J/g. In general, the slag with too low melting heat has good fluidity, which causes the heat to dissipate fast, and is not conducive to the storage heat of hearth. Too high melting heat of the slag requires higher fuel ratio to supply enough heat for the operation and results in a large heat loss in the hearth. Therefore, 0.35–0.45 of $w(MgO)/w(Al_2O_3)$ is suitable when R is 1.15–1.25, and $w(MgO)/w(Al_2O_3)$ is allowed to be a bit smaller when R is high from the view of the melting heat because the melting heat of those is between 150 J/g and 225 J/g.

4. Conclusions

In this paper, the effects of slag compositions, including $w(MgO)/w(Al_2O_3)$, basicity ($R=w(CaO)/w(SiO_2)$), and $w(Al_2O_3)$, on melting performance were studied by combining with the DSC, phase diagram, XRD, SEM-EDS, and Raman spectrum analyses. The conclusions are summarized as follows:

(1) An increase in R and $w(Al_2O_3)$ of the slag leads to an increase in the T_{end} of the blast furnace slag. For almost all slag samples in this work there is no obvious change in the T_{end} with the increase of $w(MgO)/w(Al_2O_3)$.

(2) When ($w(MgO)/w(Al_2O_3)$, R, and $w(Al_2O_3)$ are high, T_{onset} of the slag increases with the increase of one of the variables. When R is low, T_{onset} of the slag decreases with the increase of $w(Al_2O_3)$.

(3) The melting heat of the slag increases with the increase of $w(MgO)/w(Al_2O_3)$, R, and $w(Al_2O_3)$.

Author contributions

Haiyan ZHENG: Conceptualization, Methodology, Validation, Formal analysis, Investigation, Project administration, Funding acquisition; Yan ZHANG: Formal analysis, Investigation, Writing – review & editing; Zhen Wang: Formal analysis, Writing – review & editing; Jinlei DU: Data curation, Formal analysis, Investigation; Xin JIANG: Writing – review & editing; Qiangjian GAO: Writing – review & editing; Fengman SHEN: Resources, Supervision, Project administration.

Declaration of competing interest

The authors declare that they have no known competing financial interests or personal relationships that could have appeared to influence the work reported in this paper.

References

[1] H. C. Chuang, W. S. Hwang, S. H. Liu, Effects of basicity and FeO content on the softening and melting temperatures of the $CaO-SiO_2-MgO-Al_2O_3$ slag system, Material Transactions, 50 (6) (2009) 1448-1456. https://doi.org/10.2320/matertrans.MRA2008372.

[2] I. V. Flores, L. A. da Silva, N. C. Heck, M. C. Bagatini, A thermodynamic model toward the comprehension of ferrous burden softening and melting using FactSage macro-processing, Metallurgical and Materials Transactions B, 50 (2019) 2681-2693. https://doi.org/10.1007/s11663-019-01684-z.

[3] C. C. Lan, S. H. Zhang, X. J. Liu, L. Qing, M. F. Jiang, Change and mechanism analysis of the softening-melting behavior of the iron-bearing burden in a hydrogen-rich blast furnace, International Journal of Hydrogen Energy, 45 (28) (2020) 14255-14265. https://doi.org/10.1016/j.ijhydene.2020.03.143.

[4] K. X. Jiao, Z. Y. Chang, C. L. Chen, J. L. Zhang, Thermodynamic properties and viscosities of $CaO-SiO_2-MgO-Al_2O_3$ slags, Metallurgical and Materials Transactions B, 50 (2019) 1012–1022. https://doi.org/10.1007/s11663-018-1490-6.

[5] S. L. Wu, L. X. Wang, Y. N. Lu, K. Gu, Influence of high temperature interaction on the softening and melting behaviors of iron bearing materials in the blast furnace, Steel Research International, 89 (12) (2018) 1800041. https://doi.org/10.1002/srin.201800041.

[6] E. F. Osborn, R. C. DeVries, K. H. Gee, H. M. Kraner, Optimum composition of blast furnace slag as deduced from liquidus data for the quaternary system $CaO-MgO-Al_2O_3-SiO_2$, JOM, 6 (1954) 33-45. https://doi.org/10.1007/BF03397977.

[7] W. G. Kong, J. H. Liu, Z. J. He, Thermodynamic research on liquid phase formation behavior and crystallization process of blast furnace slag, Journal of Iron and Steel Research, 33 (2021) 375-384. https://doi.org/10.13228/j.boyuan.issn1001-0963.20200239.

[8] T. Umadevi, K. S. Sridhara, M. Raju, M. Basavaraja, R. Sah, S. Desai, Optimization of pellet plant straight grate induration furnace firing cycle for high alumina and high LOI iron ore pellet, Transactions of the Indian Institute of Metals 75, (2022) 3203–3212. https://doi.org/10.1007/s12666-022-02707-1.

[9] G. H. Li, M. D. Liu, T. Jiang, T. H. Zhou, X. H. Fan, Mineralogy characteristics and separation of aluminum and iron of high-aluminum iron ores, Journal of Central South University (Science and Technology), 40 (2009) 1165-1171.

[10] J. J. Dong, G. Wang, Y. G. Gong, Q. G. Xue, J. S, Wang, Effect of high alumina iron ore of gibbsite type on sintering performance, Ironmaking & Steelmaking, 42 (1) (2015) 34-40. https://doi.org/10.1179/1743281214Y.0000000195.

[11] A. Koryttseva, A. Navrotsky. High-temperature calorimetric study of oxide component dissolution in a $CaO-MgO-Al_2O_3-SiO_2$ slag at 1450° C, Journal of the American Ceramic Society, 100 (2017) 1172-1177. https://doi.org/10.1111/jace.14656.

[12] Z. M. Wang, Q. Lv, F. M. Li, S. H. Zhang, Melting performance of blast furnace slag at Handan Iron and Steel, Journal of Iron and Steel Research, 21 (05) (2009) 59-62. https://doi.org/10.13228/j.boyuan.issn1001-0963.2009.05.011.

[13] Z. D. Pang, X. W. Lv, Y. Y. Jiang, J. W. Ling, Z. M. Y, Blast furnace ironmaking process with super-high TiO_2 in the slag: viscosity and melting properties of the slag, Metallurgical and Materials Transactions B, 51 (2020) 722-731. https://doi.org/10.1007/s11663-019-01756-0.

[14] J. T. Ju, C. M. Tang, Z. G. Pang, X. D. Xing, G. H. Ji, Effect of high MgO/Al_2O_3 ratio (1.2 to 2.2) on sintering behavior and metallurgical properties. Journal of Mining and Metallurgy, Section B: Metallurgy, 57 (1) (2021) 21–30. https://doi.org/10.2298/JMMB200330034J.

[15] W. L. Zhan, Y. Liu, T. F. Shao, X. Han, Q. H. Pang, J. H. Zhang, Z. J. He, Evaluating the effect of MgO/Al_2O_3 ratio on thermal behaviors and structures of blast furnace slag with low carbon consumption. Crystals, 11 (11) (2021) 1386. https://doi.org/10.3390/cryst11111386.

[16] S. D. Mao, P. Du, Effect of reduction of MgO content in BF slag on viscosity and melting temperature, Journal of Iron and Steel Research, 27 (2015) 33-38. https://doi.org/10.13228/j.boyuan.issn1001-0963.20140245.

[17] F. M. Shen, H. Y. Zheng, X. Jiang, G. Wei, Q. L. Wen. Influence of Al_2O_3 in blast furnace smelting and discussions on proper $w(MgO)/w(Al_2O_3)$ ratio. Iron & Steel, 49 (01) (2014) 1-6. https://doi.org/10.13228/j.boyuan.issn0449-749x.2014.01.008.

[18] F. M. Shen, H. Y. Zheng, Q. J. Gao, X. Jiang, H. S. Han, F. Long, Study on MgO addition method and effect based on suitable MgO/Al_2O_3 ratio. Ironmaking. 38 (2019) 22-26.

[19] K. Sunahara, K. Nakano, M. Hoshi, T. Inada, S. Komatsu, T. Yamamoto, Effect of high Al_2O_3 slag on the blast furnace operations, ISIJ International, 48 (4) (2008) 420-429. https://doi.org/10.2355/isijinternational.48.420.

[20] L. Yao, S. Ren, X. Q. Wang, Q. C. Liu, L. Y. Dong, J. F. Yang, J. B. Liu, Effect of Al_2O_3, MgO, and CaO/SiO_2 on viscosity of high alumina blast furnace slag, Steel Research International, 87 (2016) 241-249. https://doi.org/10.1002/srin.201500021.

[21] M. Hino, Tetsuya. Nagasaka, A. Katsumata, K-I. H, K. Yamaguchi, Norimitsu. Kon-No, Simulation of primary-slag melting behavior in the cohesive zone of a blast furnace, considering the effect of Al_2O_3, Fe_tO, and basicity in the sinter ore, Metallurgical and Materials Transactions B 30, (1999) 671–683. https://doi.org/10.1007/s11663-999-0028-3.

[22] Shankar, M. Görnerup, A. Lahiri, S. Seetharaman, Experimental Investigation of the Viscosities in $CaO-SiO_2-MgO-Al_2O_3$ and $CaO-SiO_2-MgO-Al_2O_3-TiO_2$ Slags, Metallurgical and Materials Transactions B 38, (2007) 911–915. https://doi.org/10.1007/s11663-007-9087-5.

[23] K. Gao, K. X. Jiao, J. L. Zhang, Thermodynamic

properties and viscosities of high-titanium slags, ISIJ International, 60 (9) (2020) 1902-1908. https://doi.org/10.2355/isijinternational.ISIJINT-2020-004.

[24] J. Zhang, K. X. Jiao, J. L. Zhang, H. B. Ma, Y. B. Zong, Z. Y. Guo, Z. Y. Wang, Thermal stability of molten slag in blast furnace hearth, ISIJ International, 61 (8) (2021) 2227-2236. https://doi.org/10.2355/isijinternational.ISIJINT-2021-066.

[25] L. Yao, S. Ren, X. Q. Wang, Q. C. Liu, L. Y. Dong, J. F. Yang, J. B. Liu, Effect of Al_2O_3, MgO, and CaO/SiO_2 on viscosity of high alumina blast furnace slag, Steel Research International, 87 (2) (2016) 241-249. https://doi.org/10.1002/srin.201500021.

[26] F. M. Shen, X. G. Hu, H. Y. Zheng, X. Jiang, Q. J. Gao, H. S. Han, F. Long, Proper MgO/Al_2O_3 ratio in blast furnace slag: analysis of proper MgO/Al_2O_3 ratio based on observed data, Metals, 10 (6) (2020) 784. https://doi.org/10.3390/met10060784.

[27] W. G. Kong, J. H. Liu, Y. W. Yu, X. M. Hou, Z. J. He, Effect of $w(MgO)/w(Al_2O_3)$ ratio and basicity on microstructure and metallurgical properties of blast furnace slag, Journal of Iron and Steel Research International, 2 (2021) 1223-1232. https://doi.org/10.1007/s42243-021-00622-1.

[28] C. Y. Xu, C. Wang, R. Z. Xu, J. L. Zhang, K. X. Jiao, Effect of Al_2O_3 on the viscosity of $CaO-SiO_2-Al_2O_3-MgO-Cr_2O_3$ slags, International Journal of Minerals, Metallurgy and Materials, 28 (2021) 797-803. https://doi.org/10.1007/s12613-020-2187-9.

[29] T. Wu, S. P. He, Y. J. Liang, Q. Wang, Molecular dynamics simulation of the structure and properties for the $CaO-SiO_2$ and $CaO-Al_2O_3$ systems, Journal of Non-Crystalline Solids, 411 (1) (2015) 145-151. https://doi.org/10.1016/j.jnoncrysol.2014.12.030.

[30] J. G. Speight, Lange's handbook of chemistry, New York: McGraw-Hill Professional, 2005.

[31] H. Y. Zheng, L. S. Liang, J. L. Du, S. F. Zhou, X. Jiang, Q. J. Gao, F. M. Shen, Mineral transform and specific heat capacity characterization of blast furnace slag with high Al_2O_3 in heating process, Steel Research International, 92 (3) (2021) 2000448. https://doi.org/10.1002/srin.202000448.

[32] W. M. Haynes, D. R. Lide, T. J. Bruno, CRC handbook of chemistry and physics. CRC press, 2016.

PERFORMANSE TOPLJENJA ŠLJAKE VISOKE PEĆI SA VISOKIM SADRŽAJEM GLINICE

H.-Y. Zheng [a, b, *], Y. Zhang [a, b], Z. Wang [a, b], J.-L. Du [c], X. Jiang [a, b], Q.-J. Gao [a, b], F.-M. Shen [a, b]

[a] Glavna laboratorija za ekološku metalurgiju multimetaličnih minerala (Ministarstvo obrazovanja), Severnoistočni univerzitet, Šenjang, NR Kina
[b] Metalurški fakultet, Severnoistočni univerzitet, Šenjang, NR Kina
[c] Odsek za proizvodnju čelika, Šougang Jingtang Gvožđe&čelik Co., Ltd., Energetski industrijski park za gvožđe i čelik, Tangšan, NR Kina

Apstrakt

Da bi se razumele performanse šljake visoke peći sa visokim sadržajem Al_2O_3, efekti $w(MgO)/w(Al_2O_3)$, $w(CaO)/w(SiO_2)$ i $w(Al_2O_3)$ na performanse topljenja (karakteristična temperatura topljenja i toplota topljenja) šljake iz visokih peći sa visokim sadržajem Al_2O_3 su ispitivane metodom diferencijalnog skenirajuceg kalorimetra (DSC). Eksperimentalni rezultati pokazuju da konačna temperatura topljenja (T_{end}) za skoro sve šljake nema očiglednje promene sa porastom $w(MgO)/w(Al_2O_3)$, dok porast $w(CaO)/w(SiO_2)$ i $w(Al_2O_3)$ šljake povećavaju T_{end} šljake. Kada su $w(MgO)/w(Al_2O_3)$, R i $w(Al_2O_3)$ visoki, temperatura početka topljenja (T_{onset}) šljake raste sa povećanjem jedne od varijabli. Kada je $w(CaO)/w(SiO_2)$ nizak, T_{onset} šljake opada sa povećanjem $w(Al_2O_3)$. $w(MgO)/w(Al_2O_3)$, $w(CaO)/w(SiO_2)$ i $w(Al_2O_3)$ su u kontekstu ove studije i svi ovi faktori dovode do povecanja temperature topljenja šljake.

Ključne reči: Šljaka visoke peći sa visokim sadržajem glinice; Karakteristična temperatura topljenja; Toplota topljenja; Diferencijalni skenirajući kalorimetar; Ramanska spektroskopija

https://doi.org/10.1201/9781315380476.